Turbulence
Lasers, high-energy
Propagation
Phase

Method for inclusion of low-frequency contributions in numerical representation of atmospheric turbulence

B. J. Herman and L. A. Strugala

Lockheed Palo Alto Research Laboratory
3251 Hanover Street, Palo Alto, CA 94304

ABSTRACT

A standard method for calculating realizations of phase screens to simulate atmospheric turbulence for optical propagation computer codes includes only frequency information that can be represented on the discretized grid. We describe a modification to this method that can be used to include low-frequency aberrations such as tilt. We show that the modified phase screens give a better statistical representation of Kolmogorov turbulence than the unmodified phase screens. We also present comparisons of simulations using these modified phase screens to theoretical calculations of Strehl ratio with finite outer scale effects.

1. INTRODUCTION

For computer simulations of laser propagation in the atmosphere it is necessary to calculate representations of atmospheric turbulence. In a common numerical implementation of turbulence, the spatial scales that can be included in a realization are limited by the size and discretization of the computation grid. The result of this limitation is that very large spatial scales (which are responsible for low-order optical effects such as tilt) are not properly represented in a simulation. Here we describe a method for including this neglected information to give a more realistic representation of atmospheric turbulence. We begin with a review of the standard calculational method.

2. REALIZATIONS OF TURBULENCE USING SPECTRAL INFORMATION

The representation of atmospheric turbulence in wave-optics propagation codes is usually performed using a thin phase sheet approximation. The turbulent medium is discretized into several layers transverse to the direction of beam propagation. Using a split step algorithm for propagation,[1,2] a vacuum propagation step transports the beam from layer to layer while each layer contributes a phase change to the beam propagating through it. The accumulated optical phase difference for a layer of width Δz at position z_0 is given by

$$\Delta\phi(\vec{\rho}, z_0) = \frac{2\pi}{\lambda}\int_{z_0}^{z_0+\Delta z} \delta n(\vec{\rho}, z')\, dz' \quad .$$

where λ is the wavelength of the beam. We take the beam to propagate in the z direction. Optical turbulence is caused by fluctuations in the refractive index, δn.

Since the index fluctuations are statistical in nature, they can be modeled as a stochastic process. Since $\Delta\phi$ is essentially a sum over many δn's, it also can be modeled as a stochastic process which can be taken to have Gaussian statistics (by the central limit theorem) if we assume that the layer width is much larger than the correlation scale of turbulence. Thus, for implementation in a computer code of phase fluctuations due to turbulence, it is necessary to create realizations of a stochastic process with Gaussian statistics. A standard approach, based on spectral information, uses fast Fourier transforms (FFT's) for an efficient calculation.[1-3] We review this approach here.

The two-dimensional autocorrelation function of $\Delta\phi$ is defined by

$$B_{\Delta\phi}(\vec{\rho}_0 + \vec{\rho}, \vec{\rho}_0) = \langle\, \Delta\phi(\vec{\rho}_0 + \vec{\rho}, z_0)\Delta\phi(\vec{\rho}_0, z_0)\,\rangle$$

where the angular brackets denote an ensemble average. (In what follows, we will supress the dependence of quantities on the layer position, z_0.) Under the assumption of homogeneity (i.e., $B_{\Delta\phi}$ only depends on $\vec{\rho}$), this can be written in a spectral representation as

$$B_{\Delta\phi}(\vec{\rho}) = \int_{-\infty}^{\infty}\int_{-\infty}^{\infty} F_{\Delta\phi}(\vec{\kappa}_\perp)\, e^{i\vec{\kappa}_\perp\cdot\vec{\rho}}\, d\vec{\kappa}_\perp$$

where

$$F_{\Delta\phi}(\vec{\kappa}_\perp) = \frac{1}{(2\pi)^2}\int_{-\infty}^{\infty}\int_{-\infty}^{\infty} B_{\Delta\phi}(\vec{\rho})\, e^{-i\vec{\kappa}_\perp\cdot\vec{\rho}}\, d\vec{\rho}$$

is the two-dimensional power spectral density of $\Delta\phi$. This assumption also means that $\Delta\phi$ is a wide sense stationary (WSS) process.

From a well-known theorem in stochastic processes,[4] if the process $\mathbf{w}(x)$ is WSS with power spectral density $F_{\mathbf{W}}(\kappa)$ then its Fourier transform $\mathbf{W}(\kappa)$ is white noise (i.e., delta-correlated) with average intensity $F_{\mathbf{W}}(\kappa)$:

$$\langle\, \mathbf{W}(\kappa)\mathbf{W}^*(\kappa')\,\rangle = \delta(\kappa-\kappa')F_{\mathbf{W}}(\kappa).$$

Thus, since $\Delta\phi$ is WSS, we can create a realization of $\Delta\phi$ given a realization of white noise. The prescription for generating a realization of the phase change due to turbulence in a layer of width Δz is then

$$\Delta\phi(\vec{\rho}) = \int_{-\infty}^{\infty}\int_{-\infty}^{\infty} d\vec{\kappa}_\perp\, g(\vec{\kappa}_\perp)\sqrt{F_{\Delta\phi}(\vec{\kappa}_\perp)/q}\, e^{i\vec{\kappa}_\perp\cdot\vec{\rho}}. \tag{1}$$

where $g(\vec{\kappa}_\perp)$ is a two-dimensional realization of white noise with average intensity q. It also should be noted that, since $\Delta\phi(\vec{\rho})$ is real, the negative-frequency values under the integral are determined by the positive-frequency values:

$$\left[g(-\vec{\kappa}_\perp)\sqrt{F_{\Delta\phi}(-\vec{\kappa}_\perp)/q}\right]^* = g(\vec{\kappa}_\perp)\sqrt{F_{\Delta\phi}(\vec{\kappa}_\perp)/q}.$$

It remains to specify the two-dimensional power spectral density for the phase. When Δz is much larger than the correlation scale of turbulence, this is given by[5]

$$F_{\Delta\phi}(\vec{\kappa}_\perp) = 2\pi k^2\Phi_n^0(\vec{\kappa}_\perp,\kappa_z=0)\int_{z_0}^{z_0+\Delta z} C_n^2(z')\,dz' \tag{2}$$

where $k = 2\pi/\lambda$, C_n^2 is the refractive index structure constant, and $\Phi_n^0(\vec{\kappa})$ is the (scaled) refractive index power spectral density.

Under the additional assumption of isotropy, $\Phi_n^0(\vec{\kappa})$ depends only on $\kappa = (\kappa_\perp^2+\kappa_z^2)^{1/2}$. For scale lengths between the inner and outer scales of turbulence, l_0 and L_0, (i.e., in the inertial sub-range), $\Phi_n^0(\kappa)$ has the form of the Kolmogorov spectrum:[5]

$$\Phi_n^0(\kappa) = 0.033\kappa^{-11/3}. \tag{3}$$

The power spectral density is sometimes recast in a more convenient form by introducing the coherence diameter for the layer:[6]

$$r_0 = 0.185\left[\frac{\lambda^2}{\int_{z_0}^{z_0+\Delta z} C_n^2(z')\,dz'}\right]^{3/5}.$$

Then (2) becomes

$$F_{\Delta\phi}(\kappa_\perp) = 0.490 r_0^{-5/3}\kappa_\perp^{-11/3} \tag{4}$$

Using (4) in (1) gives a complete description of phase due to a turbulent layer. For computer implementation, the white noise can be obtained from a pseudo-random number generator. The integral is a Fourier transform which, if approximated by a discrete Fourier transform (DFT), can be efficiently calculated using FFT routines. Discretization of (1) then yields

$$\Delta\phi(x_m, y_n) = \frac{2\pi}{\sqrt{G_x G_y}} \sum_{m'=-N_x/2}^{N_x/2-1} \sum_{n'=-N_y/2}^{N_y/2-1} e^{2\pi i(\frac{m'm}{N_x} + \frac{n'n}{N_y})} h(f_{x_{m'}}, f_{y_{n'}}) \sqrt{0.00058 r_0^{-5/3} (f_{x_{m'}}^2 + f_{y_{n'}}^2)^{-11/6}} \quad (5)$$

where the turbulence screen is taken to have dimensions G_x by G_y, discretized into N_x by N_y points (assumed even). The points on the screen are labeled by $x_m = mG_x/N_x$ and $y_n = nG_y/N_y$, while in frequency space we have $f_{x_{m'}} = m'/G_x$ and $f_{y_{n'}} = n'/G_y$. We have converted from angular to linear frequencies in order to use the FFT algorithm ($\kappa = 2\pi f$). The complex random numbers $h(f_{x_{m'}}, f_{y_{n'}})$ in (5) are independently generated and taken to be normally distributed (zero mean, unit variance):

$$\begin{aligned} \langle h(f_{x_{m'}}, f_{y_{n'}}) \rangle &= 0 \\ \langle h(f_{x_{m'}}, f_{y_{n'}}) h^*(f_{x_{m''}}, f_{y_{n''}}) \rangle &= \delta_{m'm''}\delta_{n'n''}. \end{aligned}$$

The zero frequency value of the spectrum ($m' = 0$, $n' = 0$) must be assigned a value since it falls outside of the inertial range. It is usually taken to be zero to give an average phase of zero for a realization.

3. LOW FREQUENCY INFORMATION

Use of the FFT algorithm inherently restricts the range of frequencies that are represented on the finite size of the phase screen grid. If the coordinate grid has width G_u in the u direction (where u is either x or y) and is discretized by N_u points, then the grid is sampled at intervals $\Delta u = G_u/N_u$ by the FFT. In frequency space, the highest (linear) spatial frequency that can be sampled is then the Nyquist frequency of the grid, $1/2\Delta u$. The lowest non-zero sampled frequency is $1/G_u$. We can estimate the size of spatial scales involved by taking a representative atmospheric propagation problem.

Let us propagate a 1 m diameter beam through the atmosphere. For simplicity, we take $G_u = 1.28$ m and $N_u = 128$. Then $\Delta u = 1$ cm. We compare these lengths with the inner and outer scales. Near the ground, L_0 is on the order of the height above the ground and l_0 is on the order of 1 mm. Thus, for even moderate heights above the ground, the FFT method does not sample out to the outer scale or down to the inner scale. For the inner scale, this probably is not important because of the rapid falloff of the frequency spectrum (3): $\Phi_n^0(\kappa = 2\pi/G_u)/\Phi_n^0(\kappa = \pi/\Delta u) = (N_u/2)^{11/3} \approx 4 \times 10^6$ for $N_u = 128$. However, for low spatial frequencies, Φ_n^0 can give a large contribution to the integral in (1) and should not be ignored. This part of the spectrum contains information from spatial scales whose length is larger than the grid size and includes low-order optical effects such as tilt.

In order to properly account for the low frequency contribution to the phase screens, it is necessary to sample the spectrum at scales outside of the inertial range. In this region, the Kolmogorov spectrum no longer holds and a modified spectrum should be employed. A popular model includes a modification due to von Kármán that causes a roll over of the spectrum at the outer scale frequency:[5,7,8]

$$\Phi_n^0(\kappa) = \frac{0.033}{[\kappa^2 + L_0^{-2}]^{11/6}} \quad (6)$$

It should be pointed out that the low-frequency modification of the spectrum is a mathematical artifice to prevent (3) from becoming infinite as $\kappa \to 0$ and has no physical basis. Indeed, for spatial scales larger than L_0, turbulence no longer can be considered isotropic.

It is not difficult to show that ignoring the low frequencies in the FFT method results in poor representation of the statistics in the generated screens. The reason for this can be seen most easily from Figure 1. Here, only

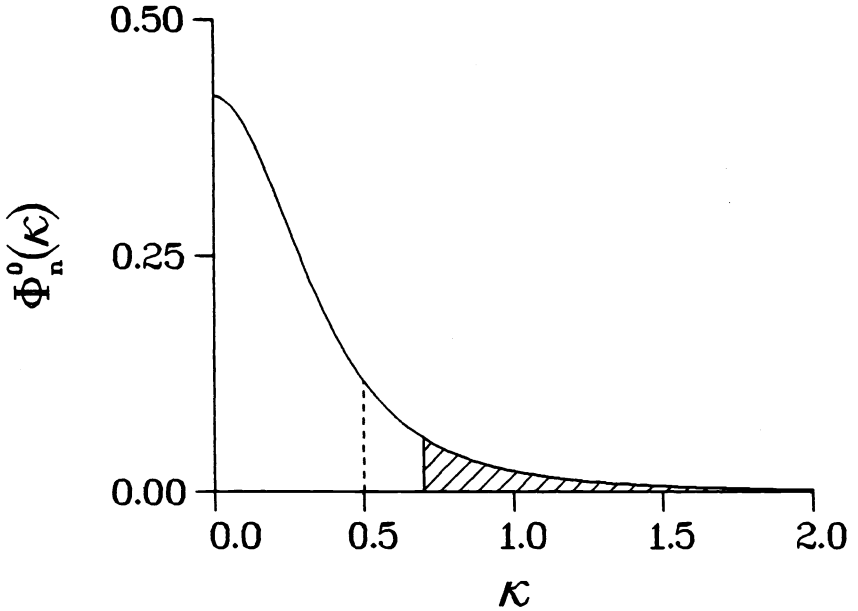

Figure 1: Plot of von Kármán spectrum (6). Shaded area corresponds to region sampled by FFT method. Dashed line corresponds to outer scale.

the part of the spectrum corresponding to the shaded area is sampled by the FFT method. In order to sample the low-frequency part of the spectrum, it is necessary to generate screens whose sizes are a few times larger than L_0. For atmospheric propagation, this calculation can become prohibitive since L_0 is generally much larger than the beam size. For example, for a 1 m diameter beam and a 10 m outer scale, we would need a grid size of about 50 m. If we require resolution on a 1 cm scale size, this implies a screen discretized by 8192 × 8192 points (assuming we use a power-of-2 FFT) for an accurate representation of turbulence. (Of course, only a small subsection of the grid would be necessary for the propagation calculation.)

4. MODIFICATION OF THE FFT METHOD FOR LOW FREQUENCIES

We desire a way of generating phase screens that contain low-frequency information without the need to create realizations on very large grids. From Figure 1, what we require is a way of calculating the contribution to the Fourier integral that comes from the unshaded part of the spectrum. An efficient way of doing this is to generate a separate phase screen via the FFT method that samples only this part of the spectrum. This "low-frequency" grid is taken to have Nyquist frequencies $1/G_x$ and $1/G_y$ in the x and y directions. In this way, the highest frequencies on this grid are matched to the lowest non-zero frequencies on the original grid. In coordinate space, this means that the cell size on the new grid is G_x by G_y, which exactly matches the full size of the original grid. Thus our original grid, which is needed for the propagation calculation, just fits inside a cell of the new grid. This is shown in Figure 2. The low-frequency grid is sampled by N_x' by N_y' points, which are not necessarily the same as N_x and N_y. If we take $5L_0$ as the largest spatial scale necessary to sample,[2] then N_x' and N_y' can be determined from $N_x' = 5L_0/G_x$ and $N_y' = 5L_0/G_y$. For our example above, this gives $N_x' = N_y' = 40$.

In order to incorporate the low-frequency information, it is necessary to add the low-frequency grid to the propagation grid at the discretization points of the propagation grid. However, the low-frequency grid is only sampled at the corners of the propagation grid, so we must perform an interpolation to obtain the required values. This interpolation must be done carefully to preserve the frequency content of the new phase screen; a simple linear interpolation will not be accurate. The proper method is by the use of trigonometric interpolating polynomials.[9] The coefficients required for the trigonometric fit are just those calculated by a DFT.[10] Since these are just the coefficients we start with when we use the spectral method, we require no additional calculation for their determination. This

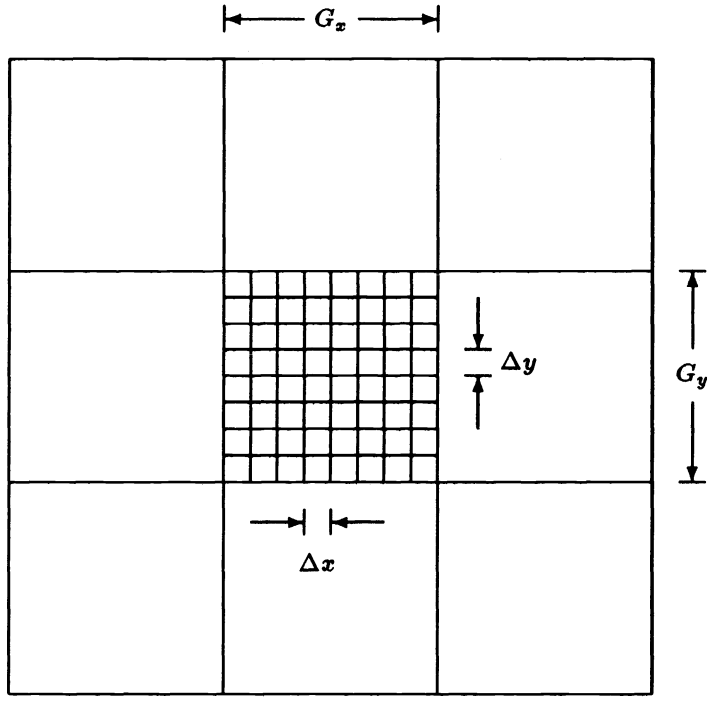

Figure 2: Relationship of low-frequency grid to propagation grid. Propagation grid is discretized into N_x by N_y points and low-frequency grid into N_x' by N_y' points. Increments on propagation grid are Δx and Δy and on low-frequency grid are G_x and G_y, where $G_x = N_x \Delta x$ and $G_y = N_y \Delta y$.

results in the following expressions: The values on the low-frequency grid are given by (assuming N_x' and N_y' to be even)

$$\Delta\phi_L(x_j, y_k) = \sum_{j'=-N_x'/2}^{N_x'/2-1} \sum_{k'=-N_y'/2}^{N_y'/2-1} e^{2\pi i\left(\frac{j'j}{N_x'} + \frac{k'k}{N_y'}\right)} \beta(f_{x_{j'}}, f_{y_{k'}})$$

where

$$\beta(f_{x_{j'}}, f_{y_{k'}}) = \frac{2\pi}{\sqrt{N_x' N_y' G_x G_y}} h(f_{x_{j'}}, f_{y_{k'}}) \sqrt{0.00058 r_0^{-5/3} (f_{x_{j'}}^2 + f_{y_{k'}}^2 + (2\pi L_0)^{-2})^{-11/6}}$$

are the Fourier coefficients. The L subscript signifies the low-frequency grid. Here, the discretization is described by $x_j = jG_x$, $y_k = kG_y$, $f_{x_{j'}} = j'/N_x'G_x$, and $f_{y_{k'}} = k'/N_y'G_y$. The trigonometric polynomial fit is given over the low-frequency grid by

$$\Delta\phi_L(x, y) = \sum_{j'=-N_x'/2}^{N_x'/2}{}' \sum_{k'=-N_y'/2}^{N_y'/2}{}' e^{2\pi i\left(\frac{j'}{N_x'G_x}x + \frac{k'}{N_y'G_y}y\right)} \beta(f_{x_{j'}}, f_{y_{k'}}) \tag{7}$$

where the primes on the sums indicate that the first and last terms are to be weighted by 1/2 and the values of β for $j' = N_x'/2$ and $k' = N_y'/2$ are the same as those for $j' = -N_x'/2$ and $k' = -N_y'/2$. The calculation of (7) requires $N_x'N_y'$ multiplications for each (x, y) point. Note that for the interpolation, we only require the Fourier coefficients, so an actual low-frequency phase screen never needs to be generated.

The values on the modified screen are obtained by combining (5) (adjusted for the von Kármán spectrum) with (7) evaluated at the points on the propagation grid:

$$\Delta\phi_{\text{mod}}(x_m, y_n) = \Delta\phi(x_m, y_n) + \Delta\phi_L(x = x_m, y = y_n).$$

We show an example of phase screens calculated by this method in Figure 3. This is a 1.28 m × 1.28 m grid where we have taken $N_x = N_y = 128$, $N_x' = N_y' = 40$, $r_0 = 10$ cm, and $L_0 = 10$ m. On the left is the phase screen generated by the usual FFT method while the modified screen is shown on the right. Note that the modified screen has low-frequency structure absent from the unmodified screen, and the screen is not periodic in the x and y directions (as it would have to be using the unmodified method).

5. STRUCTURE FUNCTION FOR THE MODIFIED PHASE SCREENS

To check how accurately the modified phase screens represent atmospheric turbulence, we must make comparisons to averaged statistical quantities. Here, the relevant quantity is the structure function, defined as the mean squared phase difference:

$$D_{\Delta\phi}(\vec{\rho}) = \langle [\Delta\phi(\vec{\rho}_0 + \vec{\rho}) - \Delta\phi(\vec{\rho}_0)]^2 \rangle. \tag{8}$$

For isotropic turbulence, this can be written using the spectral representation as[7,8]

$$D_{\Delta\phi}(\rho) = 4\pi \int_0^\infty [1 - J_0(\kappa_\perp \rho)]\, F_{\Delta\phi}(\kappa_\perp) \kappa_\perp \, d\kappa_\perp$$

where $\rho = |\vec{\rho}|$ and $J_0(\cdots)$ is the Bessel function of the first kind of order zero. For Kolmogorov turbulence, using (6), this evaluates to[8]

$$D_{\Delta\phi}(\rho) = 6.16 r_0^{-5/3} \left[\frac{3}{5} L_0^{5/3} - \frac{(\rho L_0/2)^{5/6}}{\Gamma(11/6)} K_{5/6}(\rho/L_0)\right] \tag{9}$$

where $K_{5/6}(\cdots)$ is a modified Bessel function of the third kind and $\Gamma(\cdots)$ is the gamma function. For an infinite outer scale, this reduces to the well known result

$$D_{\Delta\phi}(\rho) = 6.88\,(\rho/r_0)^{5/3}.$$

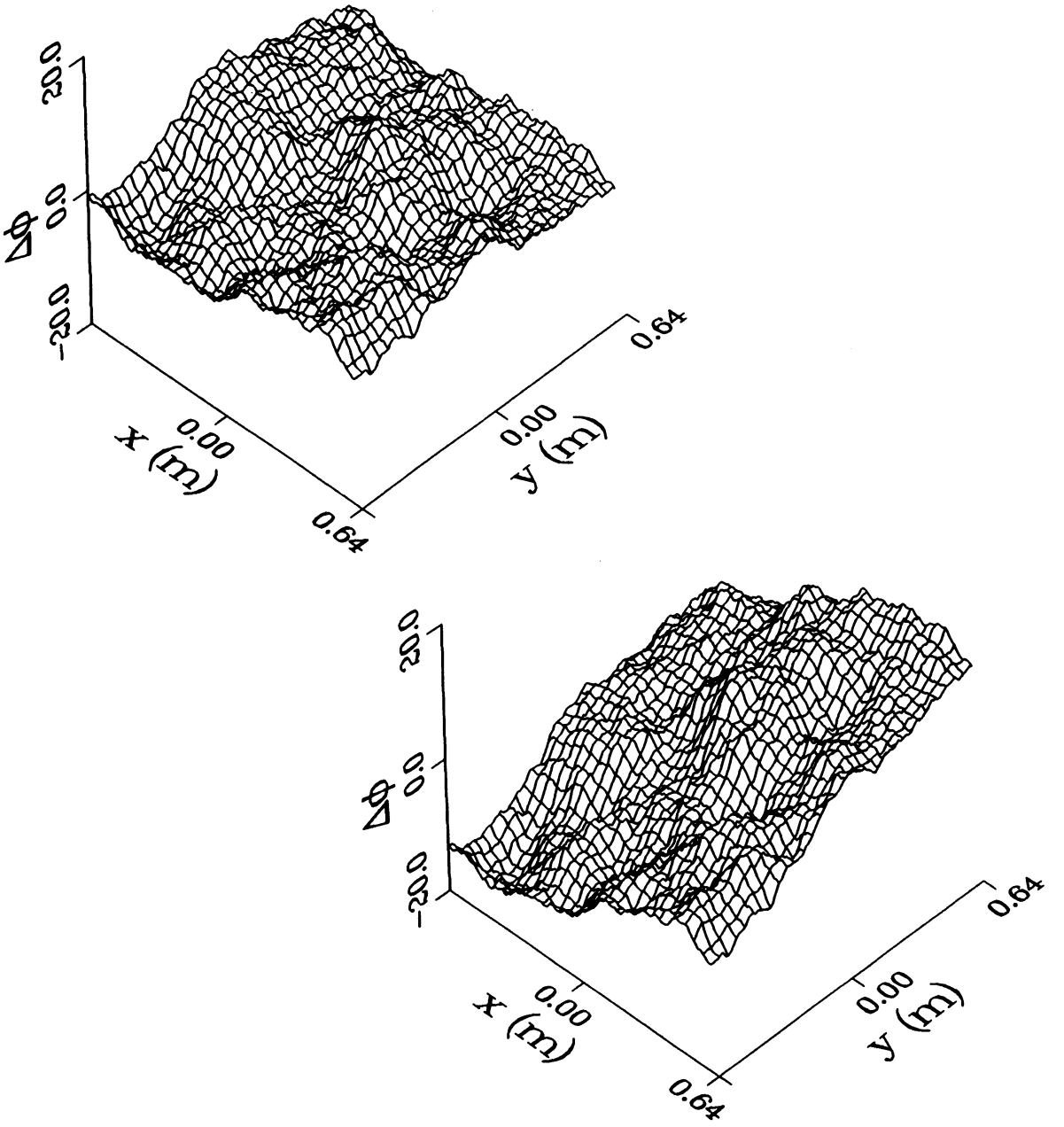

Figure 3: Sample realizations of turbulence phase screens without (left) and with (right) low-frequency modification.

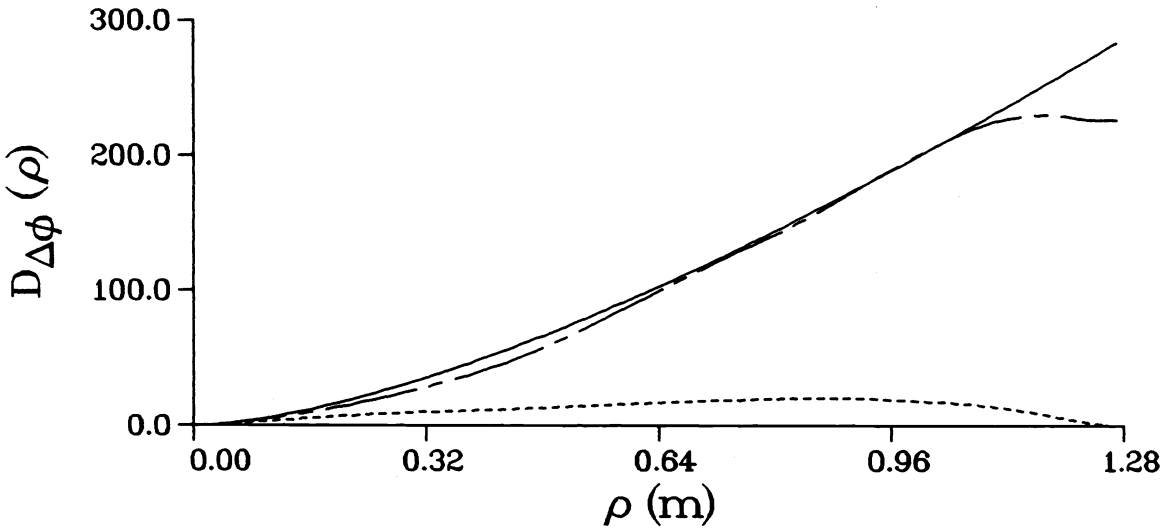

Figure 4: Comparison of reconstructed structure functions from screens in Figure 3 to theoretical values. Solid line is theory, dashed line is reconstruction from unmodified screen, chain-dashed line is reconstruction from modified screen.

According to (8) we require an ensemble average to compute the structure function. Computationally, this means we must average over several realizations of phase screens. However, since $\Delta\phi$ is WSS, we can employ the ergodic theorem[11] and replace ensemble averages by spatial averages. In our examples, therefore, we will perform averages by taking spatial averages over a single realization.

In Figure 4, we show a comparison of the theoretical structure function to the reconstructed structure functions from the screens shown in Figure 3. It can be seen that the statistics of the modified screen agree very well with theory, while those of the unmodified screen are valid only over a small range of ρ. The consequences of the periodicity of the FFT also can be seen in this figure where the value of the structure function of the unmodified phase screen approaches zero (its value at $\rho = 0$) as ρ approaches the grid size.

6. SIMULATIONS USING THE MODIFIED PHASE SCREENS

In order to check on the results obtained using the modified phase screens in wave-optics propagation codes, we must make comparisons to analytic predictions. For our investigation, we choose to use the Strehl ratio as a figure of merit. The Strehl ratio is defined to be the ratio of the peaks of the point spread functions for propagation performed with and without turbulence (i.e., a comparison of the axial peaks of the far-field intensities for turbulence propagation and diffraction-limited propagation). For propagation of a uniform beam of diameter D through isotropic turbulence, the Strehl ratio can be expressed as[8]

$$\text{S.R.} = \frac{8}{D^2}\int_0^D O_{\text{atm}}(\rho)O_{\text{ap}}(\rho)\rho\, d\rho \tag{10}$$

where

$$O_{\text{atm}}(\rho) = \exp\left[-\frac{1}{2}D_{\Delta\phi}(\rho)\right]$$

and

$$O_{\text{ap}}(\rho) = \begin{cases} \frac{2}{\pi}\left[\cos^{-1}(\rho/D) - (\rho/D)\sqrt{1-(\rho/D)^2}\right], & 0 \le \rho \le D \\ 0, & D < \rho \end{cases}$$

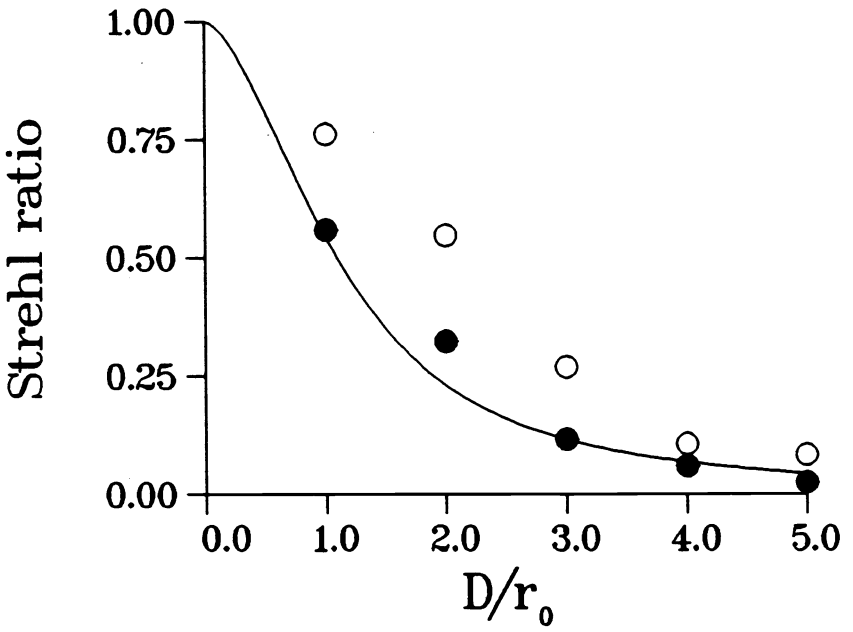

Figure 5: Comparisons of simulations to analytic results for various values of D/r_0 and $L_0/D = 10$. Solid lines show analytic Strehl ratios, hollow symbols show results using unmodified screens, filled symbols show results using modified screens.

are the optical transfer functions of the atmosphere and aperture, respectively.

For our comparison, we have simulated a propagation through the atmosphere for $L_0/D = 10$. We have taken a 0.5 m beam on a $(1.28\ \text{m})^2$ grid with $N_x = N_y = 128$ and have used the values $D/r_0 = 1, 2, \ldots, 5$. In each simulation, the r_0 for the entire propagation path was uniformly distributed into 10 layers. Each simulation was run 10 times with different initial conditions for the phase screens to obtain an averaged Strehl ratio. The results of the simulations are shown in Figure 5. The solid lines are the Strehl ratios calculated from (10) and the symbols are the results from the simulations. The filled symbols show the results using the modified screens while the hollow symbols show the results using screens generated by the usual spectral method. It is seen that using the modified screens results in much better agreement with the theory.

7. DISCUSSION

We have presented a method to modify the usual FFT method of generating phase screens for atmospheric propagation to allow for low-frequency turbulence effects. The method consists of generating realizations of turbulence on two different size grids and using a trigonometric interpolation to introduce low-frequency effects on the smaller (propagation) grid. We have shown that the phase screens generated by this method give a better representation of Kolmogorov turbulence since they include effects from the low-spatial-frequency part of the spectrum.

This method can be considerably more efficient than a straightforward implementation of the FFT method on a very large grid. If we assume a power-of-2 FFT, the straightforward implementation requires $\frac{1}{2}N_x''N_y''\log_2(N_x''N_y'')$ multiplications while the modified method requires $\frac{1}{2}N_xN_y\log_2(N_xN_y) + N_xN_yN_x'N_y'$ multiplications where N_x'' and N_y'' are the discretization numbers for the very large grid. As an example, we consider the case presented in sections 3 and 4 where $N_x'' = N_y'' = 8192$ as opposed to $N_x = N_y = 128$ and $N_x' = N_y' = 40$. We therefore have $\frac{1}{2}(8192^2 \cdot 26) \approx 8.7 \times 10^8$ multiplications for the straightforward method and $\frac{1}{2}(128^2 \cdot 14) + (128 \cdot 40)^2 \approx 2.6 \times 10^7$

multiplications for the modified method, a difference of more than an order of magnitude. Indeed, it is not difficult to show that the modified method requires fewer multiplications than the straightforward method, regardless of the criterion chosen for the maximum sampled spatial scale, as long as $N_x' N_y' > 4$. The modified method is also very memory efficient, requiring less storage than the phase screens used for the propagation simulations.

Finally, we wish to mention one application where this method may be very useful. In an experiment whose duration is long compared to the time needed for the wind to transport a section of air completely across the beam, the beam constantly sees "fresh" turbulence introduced by the wind. This is simulated in propagation codes by shifting the phase screens with the wind and using the periodicity of the FFT method to "wrap around" the turbulence. This is not entirely satisfactory since after one grid period, the beam will encounter the same turbulence. One can make the screens large (as discussed in section 3) but this brings along with it the problems of computation time and storage. The modified method provides a solution to these problems since, if one shifts both the propagation and low-frequency screens, the turbulence is fully periodic only after a period of the low-frequency screens, which can be made as large as needed for a particular simulation.

8. REFERENCES

1. J. A. Fleck, Jr., J. R. Morris, M. D. Feit, "Time-Dependent Propagation of High Energy Laser Beams through the Atmosphere," Appl. Phys. **10**, 129–160 (1976).
2. D. L. Knepp, "Multiple Phase-Screen Calculation of the Temporal Behavior of Stochastic Waves," Proc. IEEE **71**, 722–737 (1983).
3. L. E. Wittig and A. K. Sinha, "Simulation of multicorrelated random processes using the FFT algorithm," J. Acoust. Soc. Am. **58**, 630–634 (1975).
4. A. Papoulis, *Probability, Random Variables, and Stochastic Processes*, 2nd ed., p. 306 (McGraw-Hill, New York, 1984).
5. J. W. Strohbehn, "Optical Propagation through the Turbulent Atmosphere," in *Progress in Optics*, v. IX, ed. by E. Wolf, pp. 73–122, (North-Holland, Amsterdam, 1971)
6. D. L. Fried, "Optical Heterodyne Detection of an Atmospherically Distorted Signal Wavefront," Proc. IEEE **55**, 57–67 (1967).
7. R. F. Lutomirski and H. T. Yura, "Wave Structure Function and Mutual Coherence Function of an Optical Wave in a Turbulent Atmosphere," J. Opt. Soc. Am. **61**, 482–487 (1971).
8. G. C. Valley, "Long- and short-term Strehl ratios for turbulence with finite inner and outer scales," Appl. Opt. **18**, 984–987 (1979).
9. C. Lanczos, *Applied Analysis*, pp. 229–244, (Dover, New York, 1988).
10. P. Henrici, *Applied and Computational Complex Analysis*, v. 3, p. 44, (John Wiley & Sons, New York, 1986).
11. Reference 4, p. 247.